5-1-2024

Potency assay to predict the anti-inflammatory capacity of a cell therapy product for macrophage-driven diseases: Overcoming the challenges of assay development and validation

Samar Sadeghi

Laura Nimtz

Elke Niebergall-Roth

Alexandra Norrick

Stefan Hägele

See next page for additional authors

10.1016/j.jcyt.2024.02.004

Sadeghi, S., Nimtz, L., Niebergall-Roth, E., Norrick, A., Hägele, S., Vollmer, L., . . . Kluth, M. A. (2024). Potency assay to predict the anti-inflammatory capacity of a cell therapy product for macrophage-driven diseases: Overcoming the challenges of assay development and validation. Cytotherapy, 26(5), 512-523. https://doi.org/10.1016/j.jcyt.2024.02.004

Cytotherapy 26 (2024) 512–523

Contents lists available at ScienceDirect

CYTOTHERAPY

journal homepage: www.isct-cytotherapy.org

FULL-LENGTH ARTICLE
Manufacturing

Potency assay to predict the anti-inflammatory capacity of a cell therapy product for macrophage-driven diseases: overcoming the challenges of assay development and validation

Samar Sadeghi[1,#], Laura Nimtz[1,#], Elke Niebergall-Roth[1,#], Alexandra Norrick[1], Stefan Hägele[1], Lena Vollmer[1], Jasmina Esterlechner[1], Markus H. Frank[2,3,4,5], Christoph Ganss[1], Karin Scharffetter-Kochanek[6], Mark Andreas Kluth[1,*]

[1] *RHEACELL GmbH & Co. KG, Heidelberg, Germany*
[2] *Department of Dermatology, Brigham and Women's Hospital, Harvard Medical School, Boston, Massachusetts, USA*
[3] *Harvard Stem Cell Institute, Harvard University, Cambridge, Massachusetts, USA*
[4] *Transplant Research Program, Boston Children's Hospital, Harvard Medical School, Boston, Massachusetts, USA*
[5] *School of Medical and Health Sciences, Edith Cowan University, Perth, Western Australia, Australia*
[6] *Department of Dermatology and Allergic Diseases, University of Ulm, Ulm, Germany*

ARTICLE INFO

Article History:
Received 13 September 2023
Accepted 12 February 2024

Key Words:
ABCB5
immunomodulation
interleukin 1 receptor antagonist
M1 macrophages
mesenchymal stromal cells
potency assay

ABSTRACT

Background: Given the high level of product complexity and limited regulatory guidance, designing and implementing appropriate potency assays is often the most challenging part of establishing a quality control testing matrix for a cell-based medicinal product. Among the most elusive tasks are the selection of suitable read-out parameters, the development of assay designs that most closely model the pathophysiological conditions, and the validation of the methods. Here we describe these challenges and how they were addressed in developing an assay that measures the anti-inflammatory potency of mesenchymal stromal cells (MSCs) in an M1 macrophage-dominated inflammatory environment.
Methods: An *in vitro* inflammation model was established by coculturing skin-derived ABCB5$^+$ MSCs with THP-1 monocyte-derived M1-polarized macrophages. Readout was the amount of interleukin 1 receptor antagonist (IL-1RA) secreted by the MSCs in the coculture, measured by an enzyme-linked immunosorbent assay.
Results: IL-1RA was quantified with guideline-concordant selectivity, accuracy and precision over a relevant concentration range. Consistent induction of the macrophage markers CD36 and CD80 indicated successful macrophage differentiation and M1 polarization of THP-1 cells, which was functionally confirmed by release of proinflammatory tumor necrosis factor α. Testing a wide range of MSC/macrophage ratios revealed the optimal ratio for near-maximal stimulation of MSCs to secrete IL-1RA, providing absolute maximum levels per individual MSC that can be used for future comparison with clinical efficacy. Batch release testing of 71 consecutively manufactured MSC batches showed a low overall failure rate and a high comparability between donors.
Conclusions: We describe the systematic development and validation of a therapeutically relevant, straightforward, robust and reproducible potency assay to measure the immunomodulatory capacity of MSCs in M1 macrophage-driven inflammation. The insights into the challenges and how they were addressed may also be helpful to developers of potency assays related to other cellular functions and clinical indications.

Introduction

Cellular therapy products, as living cells, inherently exhibit higher heterogeneity, more limited stability, and greater molecular and mechanistic complexity than conventional drugs [1,2]. The biological activity of the cells may vary from donor to donor [3–6] and may be altered or lost during cell processing or storage [5–7]. Therefore,

* Correspondence: Mark Andreas Kluth, RHEACELL GmbH & Co. KG, Im Neuenheimer Feld 517, 69120 Heidelberg, Germany.
E-mail address: andreas.kluth@rheacell.com (M.A. Kluth).
# These authors contributed equally to this work and share first authorship.

https://doi.org/10.1016/j.jcyt.2024.02.004

mere confirmation of cell identity, quantity and viability does not necessarily guarantee the functionality of the cell therapy product [1,8]. Specific, validated potency assays are essential to ensure that the released batch is indeed capable of exerting the specific desired biological effect [8,9].

The development of appropriate potency assays is often the most challenging part of defining a testing matrix for product release [8–10]. Drug regulatory authorities require that potency assays are practical, reliable and suitable to quantify the relevant biological activity of a product related to its mode of action [11]. The assay must be able to detect meaningful changes potentially related to the clinical efficacy of the product, with predefined acceptance criteria determining whether the product can be released [1]. However, beyond basic considerations and requirements, the regulatory guidance issued by the European Medicines Agency (EMA) [12,13] and the US Food and Drug Administration (FDA) [14] does not define assay designs or read-out parameters, nor does it suggest acceptance criteria. Instead, manufacturers are required to determine appropriate potency tests specifically for each particular product [14]. The traditional approach is to design a quantitative bioassay that measures the activity of the product linked to its specific ability to elicit a clinical response in a given indication [12,14]. However, cell therapy products have multiple and often not fully characterized mechanisms of action [13,14], and the *in-vivo* conditions in the target tissue that are crucial for the product to exert its clinical effect(s) can be complex and difficult to model [1].

Mesenchymal stromal cells (MSCs) have multiple immunomodulatory properties [15–18], which have led to a widespread clinical use of these cells in several diseases characterized by dysregulated immune responses or excessive defensive inflammation [19]. Most commonly, the immunomodulatory potency of MSCs is quantified by measuring the inhibition of T cell proliferation or activation in cocultures with MSCs [9,20–22]. Potency assays targeting T cell immunity are used for release testing of MSC products for the treatment of graft-versus-host disease such as remestemcel-L [23,24] and MSC-FFM (approved in Germany as Obnitix® under the Hospital Exemption rule) [25,26].

In contrast, for clinical indications with a predominant innate immune component, it would be more appropriate to evaluate the effects of MSCs on innate immune cells, e.g. macrophages [22]. Reported assays investigating the effects of MSCs on the polarization of macrophages include *in vitro* phagocytosis assays and measurements of macrophage phenotypic surface markers or typical effector molecules [22,27]. However, for potency testing of a therapeutic product, it may not be optimal to simply adopt an *in vitro* assay that evaluates MSC functions under artificial conditions. It may be more appropriate to identify a functional marker that represents the particular *in vivo* interactions of the MSC product with the disease-specific tissue environment of the recipient [28].

In the present study we aimed to develop a potency assay that quantifies the anti-inflammatory potency of MSCs expressing ATP-binding cassette subfamily B member 5 (ABCB5$^+$ MSCs) [29], a dermal MSC population that has shown distinct immunomodulatory and wound healing-promoting effects in a variety of currently incurable skin and nonskin inflammatory diseases [30–38]. The therapeutic efficacy has been attributed in significant part to the cells' ability to release interleukin (IL)-1 receptor antagonist (IL-1RA), which can induce a phenotype switch in local macrophages from the proinflammatory M1 to the proregenerative M2 phenotype [30]. Therefore, we designed an *in vitro* inflammation model that simulates the inflammatory microenvironment of chronic skin wounds maintained by activated M1 macrophages (Figure 1), using the amount of IL-1RA secreted by ABCB5$^+$ MSCs in the stimulated macrophage-MSC coculture measured by an enzyme-linked immunosorbent assay (ELISA) as read-out. In addition to validation of the analytical method according to regulatory requirements, the potency assay was further validated and optimized with respect to underlying biological aspects, including macrophage differentiation, macrophage M1 polarization and MSC/macrophage ratio. Finally, the suitability and robustness of the potency assay for product release testing was demonstrated by testing 71 routinely manufactured MSC batches.

Materials and Methods

Cells

Human ABCB5$^+$ MSCs were expanded and isolated from dermal primary cell cultures that were derived from skin tissue samples obtained of healthy donors according to a validated Good Manufacturing Practice (GMP)-compliant protocol, as previously described [39].

Tohoku Hospital Pediatrics-1 (THP-1) cells (catalog number 300356; Cell Lines Service, Eppelheim, Germany) were cultured in suspension in RPMI 1640 medium containing 10% fetal bovine serum (FBS), 2.1 mM L-glutamine and 2.0 g/l $NaHCO_3$ (Cell Lines Service), supplemented with 100 U/mL penicillin / 100 μg/mL streptomycin (Gibco™ Penicillin-Streptomycin; Fisher Scientific, Schwerte, Germany), at 37°C, 5% CO_2, maintaining cell concentrations below 1×10^6 cells/mL.

IL-1RA secretion assay

Differentiation of THP-1 cells into macrophages

Human THP-1 cells were differentiated into macrophages by incubation in an in-house differentiation medium containing 150 nmol/mL phorbol 12-myristate 13-acetate (PMA) for 48 h at 37°C, 5% CO_2, 90% relative humidity.

Coculture of macrophages and MSCs

M1 polarization of THP-1 cell-derived macrophages was stimulated during coculture of macrophages with ABCB5$^+$ MSCs (see the Results section for the number of cells used in each experiment) in RPMI 1640 medium supplemented with 10% FBS, 2 mmol/mL L-glutamine and 100 U/mL penicillin / 100 μg/mL streptomycin by adding 50 IU/mL recombinant human interferon γ (IFN-γ) (Imukin®, Clinigen Healthcare, Schiphol, Netherlands) at the beginning of cocultivation and 50 IU/mL IFN-γ and 20 ng/mL lipopolysaccharides (LPS) from *Escherichia coli* O111:B4 (Sigma-Aldrich, Taufkirchen, Germany) at 24 h. Unstimulated MSC/macrophage cocultures and macrophage cultures without ABCB5$^+$ MSCs were used as controls. After 48 h of coculture, supernatants were collected for IL-1RA analysis.

Flow cytometric marker analysis

Differentiation and polarization of THP-1 cells into M1 macrophages was confirmed by flow cytometric (CytoFLEX S; Beckman Coulter, Krefeld, Germany) determination of the macrophage differentiation marker CD36 (as a recognized marker for the differentiation of THP-1 cells into macrophages [40–50]) and the M1 macrophage marker CD80 in THP-1 cells and THP-1-derived M1 macrophages using antibodies as specified in supplementary Table 1. Unstained THP-1 cells and isotype-FITC/isotype-AlexaFluor647-stained THP-1 cells were used as negative controls. Sufficient differentiation and M1 polarization were assumed if at least 50% of the macrophages expressed CD36 and CD80, while no more than 5% of THP-1 cells and the negative controls expressed these markers.

ELISA

After 48 h of coculture of macrophages and ABCB5$^+$ MSCs, culture supernatants were assayed for IL-1RA by a colorimetric sandwich ELISA using the Human IL-1RA/IL-1F3 Quantikine® ELISA kit (Bio-Techne, Wiesbaden, Germany). The IL-1RA ELISA was validated in accordance with the guidelines on bioanalytical method validation issued by the EMA [51] and the FDA [52], recently superseded by the International Council for Harmonisation of Technical Requirements

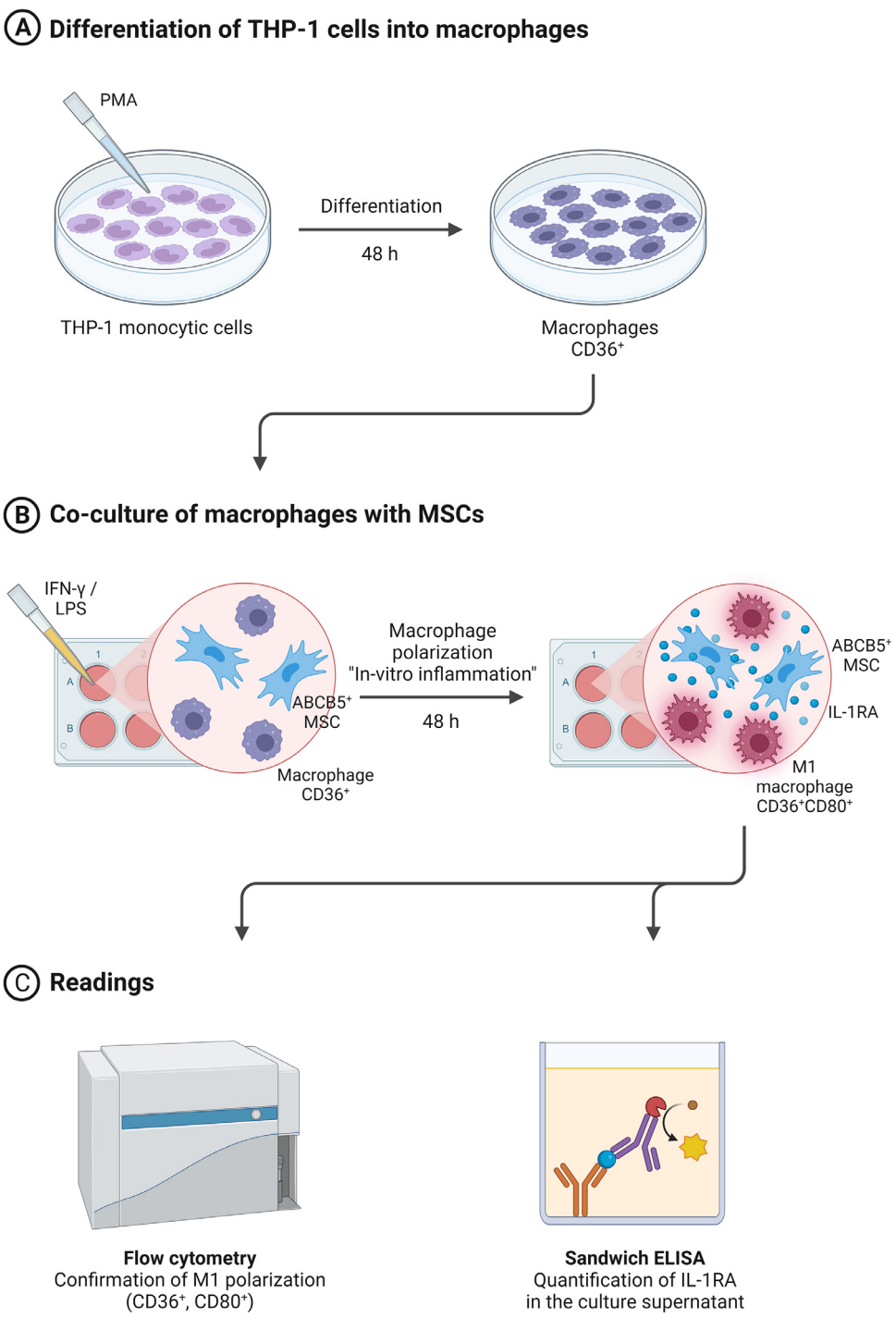

Fig. 1. Design of the IL-1RA potency assay. (A) THP-1 monocytes are differentiated into macrophages by incubation with PMA. (B) Macrophages are cocultured with ABCB5$^+$ MSCs and polarized into M1 macrophages by stimulation with IFN-γ and LPS. (C) Successful M1 polarization is confirmed by flow cytometry, and IL-1RA concentration in the coculture supernatant is determined by a colorimetric ELISA. Created with BioRender.com. (Color version of figure is available online.)

for Pharmaceuticals for Human Use (ICH) Guideline M10 on Bioanalytical Method Validation [53,54], by evaluating the parameters calibration curve, within-run and between-run precision and accuracy, total error, and selectivity against the acceptance criteria specified in the guidelines. Based on previous in-house experiences using the Human IL-1RA/IL-1F3 Quantikine® ELISA kit, 125 pg/mL was considered the anticipated lower limit of quantification (LLOQ).

Seven (4000–62.5 pg/mL; for ELISA method validation) or six (4000–125 pg/mL; for validation of analytical ELISA runs) calibration standards were prepared by serial dilution of the recombinant human IL-1RA standard solution provided in the test kit. Five (4000, 3000, 1500, 250, and 125 pg/mL; for ELISA method validation) or three (3000, 1500, and 250; for validation of analytical ELISA runs) QC samples were prepared by spiking the required amount of the IL-1RA standard solution to the sample matrix (coculture medium). In addition, to assess potential matrix effects for ELISA method validation, two individual batches of the coculture medium (diluted 1:10) were spiked at the anticipated LLOQ (125 pg/mL). Calibration diluent (assay buffer) was used as blank samples. Each 100 μl of the calibration standards (1:20), QC samples (1:20), matrix samples (coculture medium, 1:20) or analytical samples (macrophage/MSC coculture supernatant, diluted as necessary) was analyzed. Absorbance was

measured by determining the optical density (OD) at 450 nm with 620 nm reference subtraction on an Infinite® F50 Robotic microplate absorbance reader (Tecan, Crailsheim, Germany).

Calibration curves were constructed using Magellan Tracker V7.5 data analysis software (Tecan, Crailsheim, Germany) by plotting the blank-subtracted OD value (y) versus the concentration of the calibration standards (x) on a logarithmic scale. Curve fitting was achieved by four-parameter logistic regression using the Levenberg–Marquardt algorithm. The regression curve is described by the following equation:

$$y = d + \frac{a-d}{1+\left(\frac{x}{c}\right)^b}$$

where a is the lower asymptote (minimum signal), b is the slope, c is the log concentration at the inflection point (at half-maximum signal) and d is the upper asymptote (maximum signal). For (back-) calculation of the IL-1RA concentration, the equation was rearranged to isolate x:

$$x = c\left(\frac{a-d}{y-d}-1\right)^{\frac{1}{b}}$$

Results

ELISA validation

Calibration curves

Seven calibration standards over a range of 4000 pg/mL as the anticipated upper limit of quantification (ULOQ) to 62.5 pg/mL were assayed in duplicate in six independent runs on separate days. The regression parameters of the calibration curves are displayed in Table 1.

In runs 1, 2, 4, and 6, all replicates met the acceptance criteria for accuracy, defined as a bias of the back-calculated IL-1RA concentration (shown in supplementary Table 2) from the nominal concentration ≤ 20% (≤ 25% at LLOQ and ULOQ) (Table 2).

In Run 3, both replicates of Standard 7 (nominal concentration 62.5 pg/mL) were above the maximum acceptable bias of 25% (39.9% and 36.4%). For this reason, Standard 7 was rejected and a new calibration curve without Standard 7 was generated. This was permissible because Standard 7 was beyond the quantification range of the curve (below the LLOQ). On re-back-calculation (supplementary Table 2), both replicates of Standard 6 (nominal concentration 125 pg/mL) were above the maximum acceptable bias of 25% (28.1% and 29.3%) (Table 2). Since Standard 6 represented the anticipated LLOQ, Run 3 had to be excluded from further evaluation.

In Run 5, the OD values for Standard 1 (nominal concentration 4000 pg/mL) were above the OD limit of the detector ("overflow"). Therefore, a calibration curve was generated for Run 5 over the concentration range of Standards 2–7 (2000–62.5 pg/mL). This curve did not span the full concentration range, but met the guideline requirements because it included six calibration standards. Over the concentration range of 2000–62.5 pg/mL, all replicates were below the maximum acceptable bias of 20% or 25% (bias range 0.7–7.0%) (Table 2).

Overall, five calibration curves (of Runs 1, 2, 4, 5, and 6) met the criteria of at least 75% of all replicates per run and at least 50% of the replicates of each standard sample showing an acceptable accuracy and were therefore considered valid (Table 2).

Within-run evaluation

In addition to determining the within-run accuracy during generation of the calibration curves, within-run accuracy and precision were determined by analyzing five quality control (QC) samples. QC samples included the anticipated ULOQ (nominal concentration 4000 pg/mL), high QC (3000 pg/mL), medium QC (1500 pg/mL), low QC (i.e., less than three times the LLOQ, 250 pg/mL) and LLOQ (125 pg/mL) and were assessed each with five replicates. The evaluation was based on the results obtained in the five valid runs (Runs 1, 2, 4, 5, and 6; the back-calculated concentrations are shown in supplementary Table 3).

In Run 5, 4 of the 5 replicates of the ULOQ sample were above the OD limit of the detector ("overflow"). Therefore, for this sample (n = 1) precision could not be evaluated (Table 3). All but two (low QC and LLOQ in Run 4) of the QC samples met the acceptance criteria for accuracy, and all but one (LLOQ in Run 4) of the QC samples met the acceptance criteria for precision (Table 3).

Between-run evaluation

The between-run evaluation was based on the results of the five QC samples from the five valid runs (Runs 1, 2, 4, 5, and 6). All QC samples fulfilled the acceptance criteria for between-run accuracy, i.e., bias ≤ 20% (≤ 25% at LLOQ and ULOQ), between-run precision, i.e., coefficient of variation (CV) ≤20% (≤25% at LLOQ and ULOQ), and total error, i.e., ≤30% (≤40% at LLOQ and ULOQ) (Table 3).

Selectivity

Selectivity, defined as the ability of the assay to measure the analyte of interest in the presence of unrelated compounds of the matrix,

Table 1
Regression parameters of the calibration curves of the IL-1RA ELISA.

Run	Lower asymptote (minimum signal)	Slope	Log concentration at the inflection point	Upper asymptote (maximum signal)
1	0.0016984	1.0448	218,110	235.95
2	0.005932	1.1073	310,830	427.75
3	−0.005305	1.1264	42,116	48.525
3 (S1–S6)[a]	−0.029049	1.0652	2,839,900	3511.8
4	0.0084542	1.1326	14,705	18.518
5[b]	0.010277	1.1337	12,533	16.181
6	−0.005948	1.0652	369,560	382.72

Calibration curves were generated by measuring the OD of seven calibrations standards (S1–S7; 4000, 2000, 1000, 500, 250, 125, and 62.5 pg/mL IL-1RA) assayed in duplicate in six independent runs on separate days. Curve fitting was achieved by four-parameter logistic regression using the Levenberg–Marquardt algorithm.

[a] Since in Run 3 both replicates of the standard S7 (62.5 pg/mL) were above the maximum acceptable bias, a new calibration curve was generated without S7.

[b] OD values for the highest calibration standard (4000 pg/mL) were above the OD limit of the detector. Therefore, the calibration curve of Run 5 covers a calibration range of 2000–62.5 pg/mL.

Table 2
Accuracy of the calibration standard measurements of the IL-1RA ELISA.

		Standard sample nominal IL-1RA concentration (pg/mL)							
		S1	S2	S3	S4	S5	S6	S7	Run valid?[b]
		4000 (ULOQ)	2000	1000	500	250	125 (LLOQ)	62.5	
Acceptance criterion[a]		≤ 25	≤ 20	≤ 20	≤ 20	≤ 20	≤ 25	≤ 25	
Run 1	R1	2.8	1.0	2.2	1.9	1.1	1.1	2.7	Yes
	R2	2.8	0.7	3.8	0.8	4.2	5.7	1.0	
Run 2	R1	4.2	0.5	1.3	3.5	1.2	2.1	0.2	Yes
	R2	4.2	0.3	3.1	1.4	1.5	4.0	4.7	
Run 3	R1	1.2	0.2	3.6	0.1	31.7	15.3	39.9	No
	R2	1.3	1.1	2.2	1.1	18.9	16.6	36.4	
Run 3	R1	1.2	0.0	3.0	0.3	26.2	28.1	n.a.[c]	No
(S1 – S6)[c]	R2	1.3	1.0	1.6	0.7	14.4	29.3	n.a.[c]	
Run 4	R1	0.4	1.2	5.1	15.9	0.4	4.5	10.1	Yes
	R2	0.5	0.1	1.8	1.6	1.1	5.7	7.0	
Run 5	R1	n.d.[d]	1.8	0.8	0.8	2.2	0.9	7.0	Yes
	R2	n.d.[d]	1.8	0.7	1.2	2.0	3.4	2.8	
Run 6	R1	3.3	2.5	1.3	5.7	5.7	0.9	18.5	Yes
	R2	3.3	1.4	4.7	2.1	7.7	8.7	17.2	

Accuracy is given as % bias of the back-calculated concentration from the nominal concentration. The back-calculated IL-1RA concentrations are given in supplementary Table 2.
n.a., not applicable; n.d., not determined; R, replicate; S, standard sample.
[a] As defined in the EMA's and FDA's guidelines on bioanalytical method validation [51–54]; i.e., ≤20% (≤25% at the ULOQ and LLOQ).
[b] According to the criteria defined in the EMA's and FDA's guidelines on bioanalytical method validation [51–54]; i.e., ≥6 standard samples run at least in duplicate, with ≥75% of replicates per run and ≥50% of replicates per standard sample showing acceptable accuracy.
[c] Since in Run 3 both replicates of S7 were above the maximum acceptable bias, a new calibration curve was generated without S7.
[d] OD value was above the OD limit of the detector ("overflow").

was assessed on matrix samples prepared from the coculture medium spiked at the LLOQ (125 pg/mL). Since the matrix is a chemically defined medium, testing of at least ten matrices, as required by the EMA's and FDA's guidelines, was waived and instead two batches of the culture medium were tested with five replicates each. The evaluation was based on the results obtained in the five valid runs (Runs 1, 2, 4, 5, and 6) with a total of 50 replicates (supplementary Table 4).

In total, 6 of the 50 replicates (2 in Run 1 and 4 in Run 4) had a bias >25% (maximum 33%), while 44/50 (88%) of replicates had a bias

Table 3
Accuracy, precision, and total error of the IL-1RA ELISA.

		Quality control sample Nominal IL-1RA concentration (pg/mL)				
		ULOQ	High QC	Medium QC	Low QC	LLOQ
		4000	3000	1500	250	125
Accuracy[a] (% bias)	Run 1	6.9[b]	2.8	4.4	17.6	12.6
	Run 2	4.9	2.8	5.7	7.2	6.1
	Run 4	11.2	19.8	17.0	20.7	32.2
	Run 5	7.4[c,d]	4.8[d]	10.9	11.7	9.3
	Run 6	2.7	4.0	4.4	8.3	5.7
	Between-run	0.4	5.4	7.4	11.8	8.6
	Acceptance criterion[e]	≤ 25	≤ 20	≤ 20	≤ 20	≤ 25
Precision (% CV)	Run 1	2.7[b]	3.6	5.5	4.7	4.9
	Run 2	3.7	3.1	3.7	6.8	9.3
	Run 4	1.5	2.4	1.9	4.5	38.9
	Run 5	n.a.[c]	5.8[d]	5.6	7.1	6.1
	Run 6	2.9	4.5	5.6	9.3	7.2
	Between-run	7.7	8.7	7.8	10.0	16.9
	Acceptance criterion[e]	≤ 25	≤ 20	≤ 20	≤ 20	≤ 25
Total error[f] (%)	Between-run	8.2	14.1	15.3	21.8	25.3
	Acceptance criterion[e]	≤ 40	≤ 30	≤ 30	≤ 30	≤ 40

Evaluation was based on the 5 runs with a valid calibration curve (Runs 1, 2, 4, 5, and 6) with 5 replicates each.
n.a., not applicable; QC, quality control sample.
[a] Bias (%) of the mean back-calculated concentration (given in supplementary Table 3) from the nominal concentration.
[b] n = 4; OD value for 1 of the 5 replicates was above the OD limit of the detector ("overflow").
[c] n = 1; OD values for 4 of the 5 replicates were above the OD limit of the detector ("overflow").
[d] Since the nominal concentration was outside the range of the calibration curve for Run 5 (see Table 2), the calculated concentration was extrapolated.
[e] As defined in the EMA's and FDA's guidelines on bioanalytical method validation [51–54].
[f] According to the EMA's and FDA's guidelines on bioanalytical method validation [51–54] defined as sum of between-run bias and CV. CV, coefficient of variation.

Table 4
Recovery of IL-1RA in sample matrix.

	Matrix sample Nominal IL-1RA concentration (pg/mL)									
	Matrix sample 1					Matrix sample 2				
	125 pg/mL (LLOQ)					125 pg/mL (LLOQ)				
	R1	R2	R3	R4	R5	R1	R2	R3	R4	R5
Run 1	27.5	24.8	28.2	24.8	22.6	24.0	22.6	21.5	18.5	14.7
Run 2	13.2	11.0	1.0	1.4	1.6	21.5	9.7	16.2	9.5	7.5
Run 4	31.0	26.4	33.0	24.9	20.1	25.9	24.4	19.4	7.4	1.3
Run 5	19.6	20.9	20.8	11.8	11.5	19.1	14.4	13.6	7.7	8.2
Run 6	7.1	8.2	1.9	5.9	8.9	3.8	8.3	7.1	11.0	11.2

Recovery was assessed on matrix samples prepared from two individual batches of the coculture medium spiked at the LLOQ. Since the matrix is a chemically defined culture medium, testing of at least ten matrices, as required by the EMA's and FDA's guidelines [51–54], was waived and instead two batches of the culture medium were tested with five replicates each. Evaluation was based on the 5 runs with a valid calibration curve (Runs 1, 2, 4, 5, and 6). Values represent accuracy, expressed as % bias of the back-calculated IL-1RA concentration from the nominal concentration. The back-calculated concentrations are given in supplementary Table 4.
R, replicate.

below 25% (Table 4). Therefore, the acceptance criterion for assay selectivity of at least 80% of replicates showing an acceptable accuracy (bias ≤25% at the LLOQ) was met, showing that the sample matrix had no relevant influence on the recovery of IL-1RA.

Biological aspects

Macrophage differentiation and M1 polarization

In eight cultures of macrophages that were differentiated from THP-1 cells and stimulated by IFN-γ and LPS, CD36 was expressed by 62.5–76.0% (mean 69.5%) and CD80 by 52.3–72.7% (mean 63.3%) of the cells. All cultures meet the acceptance criteria for macrophage differentiation and M1 polarization of 50% of cells expressing CD36 and 50% of cells expressing CD80 (Figure 2A). Validation experiments in 20 independent cultures measuring the expression of both markers simultaneously showed that 76.2% (SD 5.2%) of CD36-expressing cells were also positive for CD80 (supplementary Table 5).

In addition, M1 polarization of IFN-γ/LPS-stimulated THP-1-derived macrophages was confirmed by the detection of the proinflammatory cytokine tumor necrosis factor (TNF)-α in the culture supernatants of nine macrophage cultures, whereas no TNF-α signal was detected in cultures of unstimulated THP-1-derived macrophages and untreated THP-1 cultures (Figure 2B).

Influence of the MSC/macrophage ratio

To determine the optimal ratio between the MSCs and the macrophages as their stimulators, the influence of different MSC/macrophage ratios (range 1:1 to 1:83.3; see supplementary Table 6 for the cell numbers used) on the IL-1RA secretion was tested (Figure 3A–C). Over the entire range of ratios tested, the proportion of IL-1RA secreted by ABCB5$^+$ MSCs out of the total amount of IL-1RA measured in the culture supernatant decreased with decreasing percentages of MSCs in the coculture, ranging from 53.4% at an MSC/macrophage ratio of 1:1 down to approximately 25.2% at an MSC/macrophage ratio of 1:83.3 (Figure 3D). In contrast, the IL-1RA concentration per individual MSC increased with increasing macrophage excess (Figure 3E). A sectional regression analysis of the ratio-response curve (Figure 3F) suggested a linear increase in IL-1RA secretion per MSC up to an MSC/macrophage ratio of 1:50 (slope = 0.0326), whereas at MSC/macrophage ratios above 1:50, the curve markedly flattened (slope = 0.0135). This suggested that at an MSC/macrophage ratio of 1:50 the ratio-response curve approached a plateau. Above this ratio, the influence of the macrophage number on IL-1RA secretion by individual MSCs diminished. Therefore, an MSC/macrophage ratio of 1:50 was chosen for the IL-1RA potency assay as batch release test.

Batch release tests

In GMP batch release tests, a total of 71 MSC batches manufactured from skin tissues from six donors were tested for their potency to release IL-1RA in coculture with THP-1-derived IFN-γ/LPS-stimulated macrophages at an MSC/macrophage ratio of 1:50 (10,000 ABCB5$^+$ MSCs and 500,000 macrophages). Validity and acceptance criteria are summarized in Figure 4.

IL-1RA concentration attributable to the MSCs, defined as total concentration in the coculture supernatant minus the concentration measured in the culture supernatant of control cultures of stimulated macrophages without MSCs, ranged from 4166 to 26,176 pg/mL. Of the 71 batches, 66 (93%) met the acceptance criterion for batch release of an IL-1RA concentration of at least 6055 pg/mL (Figure 5). Donor medians ranged from 5371 to 19,078 pg/mL, with no statistically significant differences between donors. However, in contrast to Donors 1–5, the median value of Donor 6 (5371 pg/mL) was below the threshold level for batch release (6055 pg/mL), with 3 of 4 (75%) of batches failing the acceptance criterion (Figure 5).

Discussion

Potency testing is considered a key component of a sound development and quality control for advanced-therapy medicinal products, and developing and implementing appropriate potency assays is often at the center of several challenges and discussions between manufacturers and regulatory authorities [55]. Regulatory expectations include that potency assays should be representative of the mode of action, accurate, sensitive enough to detect meaningful changes, predictive of the clinical efficacy, and provide quantitative results that allow product release per defined acceptance criteria and ensure batch-to-batch consistency [55]. However, while both the EMA and the FDA have set out general considerations and principles for potency testing of cell-based medicinal products [12–14], they do no propose cell type- or disease-specific tests [10,11,21]. Rather, manufacturers are required to design an assay strategy based on the individual product's attributes [9–11,44].

One of the most challenging aspects of potency assay development is the definition of a suitable readout parameter [10,21]. The therapeutic efficacy of ABCB5$^+$ MSCs in wound healing has been primarily attributed to the induction of an immunophenotype shift in

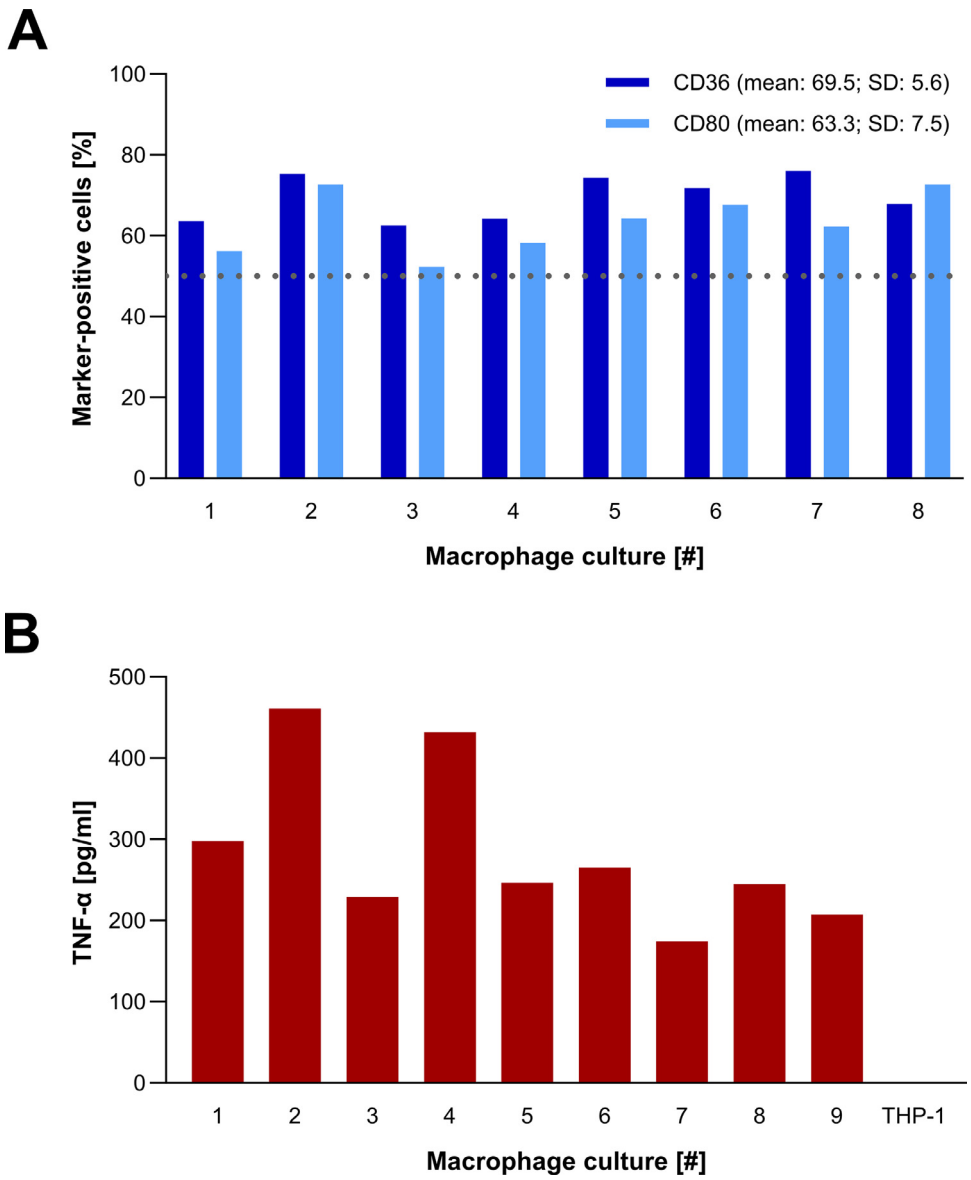

Fig. 2. Assessment of differentiation and M1 polarization of THP-1-derived macrophages. (A) Expression of the macrophage differentiation marker CD36 and the M1 marker CD80 on macrophages that were differentiated from THP-1 cells and stimulated by IFN-γ and LPS. The dotted line marks the acceptance level for both markers, above which sufficient differentiation and M1 polarization was assumed. (B) TNF-α concentration in the culture supernatant of IFN-γ/LPS-stimulated THP-1-dervived macrophage cultures determined by ELISA (using the Invitrogen TNF alpha Human ELISA Kit, KHC3011, Thermo Fisher Scientific, Darmstadt, Germany). In cultures of untreated THP-1 cells (right), no TNF-α signal was detected. (Color version of figure is available online.)

local wound macrophages from a proinflammatory M1 to a proregenerative M2 phenotype [30]. This effect can be functionally mirrored in cocultures of ABCB5$^+$ MSCs and activated macrophages, where the macrophages release significantly less proinflammatory cytokines TNF-α and IL-12/IL-23p40 and significantly more anti-inflammatory IL-10 into the culture medium as compared to macrophages that are cocultured with ABCB5-depleted dermal cells or cultured alone [30]. However, although changes in parameters related to the functionality of responder cells have been frequently used as readouts for MSC potency testing, it has been assumed that the effects of MSCs on the cytokine production by immune cells *in vitro* may not readily predict the immunomodulatory efficacy of MSCs *in vivo*. This is because the clinical outcome depends not only on the amounts of cytokines produced, but also on when they are produced and for how long [9,21].

For indications where M2 macrophages play an essential role in symptom improvement, it was therefore suggested to measure instead MSC parameters that have been found related to M2 macrophage polarization, such as indoleamine 2,3-dioxygenase activity or CCL2 expression [28]. For ABCB5$^+$ MSCs, adaptively released IL-1RA has been identified as a key factor that triggers the M1-to-M2 macrophage switch. In addition, IL-1RA response to M1 macrophages is a biological property of ABCB5$^+$ MSCs that is critical for inducing their intended therapeutic effect, namely promotion of wound healing, *in vivo* [30]. This qualifies IL-1RA as a relatively easily measurable readout parameter that can reasonably be expected to be predictive the immunomodulatory and wound healing-promoting efficacy of therapeutically administered ABCB5$^+$ MSCs.

After selecting IL-1RA as the readout parameter, an ELISA-based detection method was implemented and validated to ensure reliable and reproducible readings, closely following the EMA's and FDA's guidelines on bioanalytical method validation [51–54]. Because the Human IL-1RA/IL-1F3 Quantikine® ELISA kit was validated by the manufacturer for research use only, and not for pharmaceutical use such as drug development and manufacturing, the drug regulatory

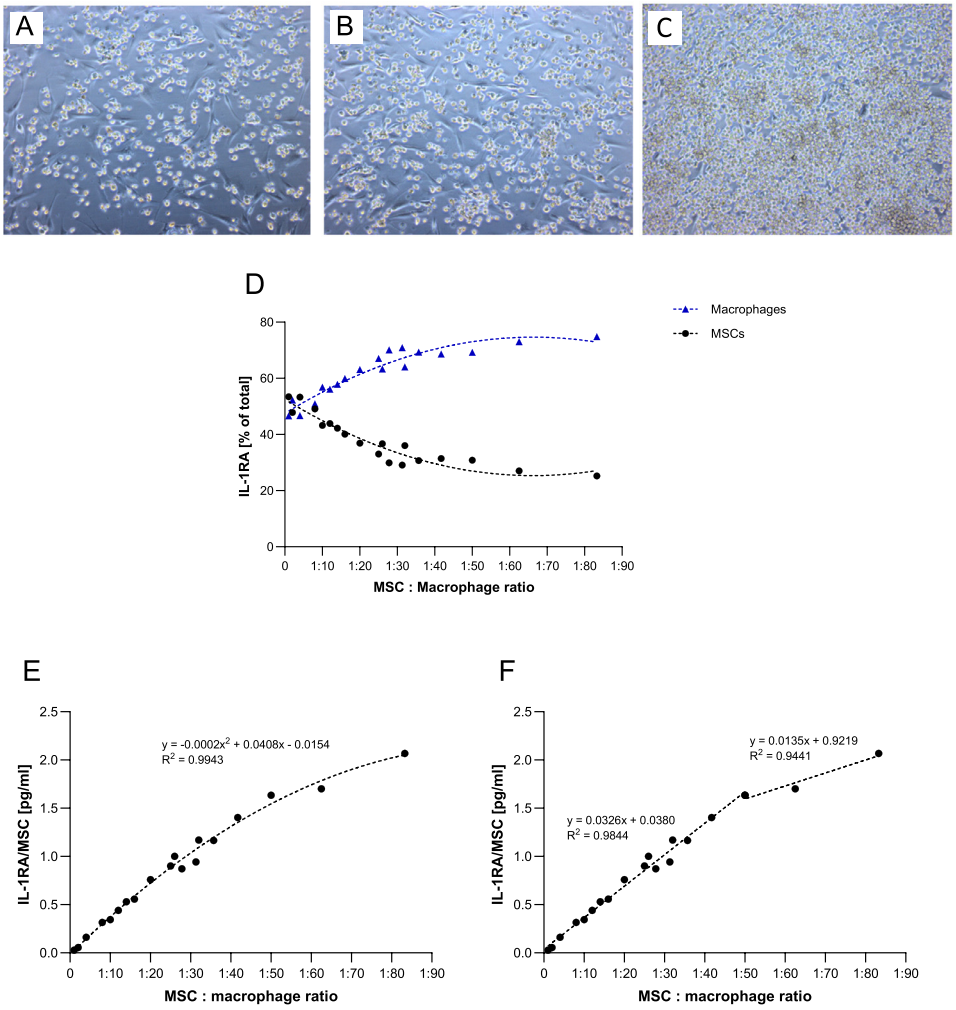

Fig. 3. Relationship between MSC/macrophage ratio and IL-1RA secretion by ABCB5$^+$ MSCs in cocultures stimulated with IFN-γ and LPS. (A–C) Light microscopy images of cocultures of ABCB5$^+$ MSCs and THP-1-derived macrophages at MSC/macrophage ratios of (A) 1:4 (20,000 MSCs and 80,000 macrophages), (B) 1:12 (20,000 MSCs and 240,000 macrophages), and (C) 1:50 (10,000 MSCs and 500,000 macrophages). (D) IL-1RA secretion by ABCB5$^+$ MSCs and macrophages as percentage of total IL-1RA in stimulated cocultures at different ABCB5$^+$ MSC/macrophage ratios. (E) IL-1RA secretion per MSC as a function of the MSC/macrophage ratio. (F) Sectional analysis of the ratio-response curve shown in (E), suggesting a linear increase in IL-1RA secretion per MSC up to an MSC/macrophage ratio of 1:50, whereas at MSC/macrophage ratios above 1:50, the curve markedly flattens. Data points represent means of 3 or 6 cocultures per MSC/macrophage ratio studied (see supplementary Table 6 for details). (Color version of figure is available online.)

guidelines required full revalidation of the kit at the site where the sample analyses are performed. By meeting all applicable acceptance criteria, it was demonstrated that the applied protocol is suitable for the quantification of IL-1RA in cell culture supernatants with guideline-concordant selectivity, accuracy and precision in the range of 125 (LLOQ) to 4000 (ULOQ) pg/mL.

In the context of developing an immunopotency assay, it is important to consider that MSCs are not constitutively immunosuppressive but require an inflammatory environment to exert their anti-inflammatory functions [9]. Consistent with this, unstimulated ABCB5$^+$ MSCs do not produce IL-1RA, but release significant amounts of IL-1RA when they are cocultured with M1 macrophages [30], which resembles the inflammatory microenvironment of chronic skin wounds *in vitro* [56]. While most commonly monocytes derived from peripheral blood mononuclear cells (PBMCs) are used to generate macrophages *in vitro* [57], in the present potency assay the inflammatory microenvironment was simulated using macrophages differentiated from THP-1 cells. Upon differentiation with PMA, THP-1 cells acquire a macrophage-like phenotype that mimics primary human macrophages in several aspects [57], making PMA-differentiated THP-1 macrophages a suitable simplified model to study M1 macrophage immune responses *in vitro* [48,58]. A major advantage of THP-1-derived over PBMC-derived macrophages is the homogeneous genetic background of the THP-1 cell line, which prevents that variations in assay readout parameters are induced or confounded by donor-dependent phenotypic variations of the macrophages [58]. Although the acceptance criteria for macrophage differentiation and M1 polarization of 50% of cells expressing CD36 and CD80, respectively, may seem low, the actual mean percentage of 63.3% CD80$^+$ cells (Figure 2A) is in the range of the percentages reported by other investigators using THP-1-differentiated M1-polarized macrophages of 45–85% [57,59–61] (for CD36, to our knowledge, no published data are available). Even more important in the context of potency assays is the uniformity of the percentages (as reflected by low standard deviations) of marker-expressing cells measured across cocultures. The consistent induction of macrophage marker expression in THP-1 cells (Figure 2A) and secretion of the proinflammatory cytokine TNF-α in THP-1-derived macrophages (Figure 2B) confirmed the suitability of the differentiation and polarization protocol described here.

Another aspect we addressed was the optimization of the ratio between the MSCs and the macrophages as their stimulators. It seems reasonable to assume that an ideal ratio of MSCs to macrophages would be that which would occur with therapeutic application of the

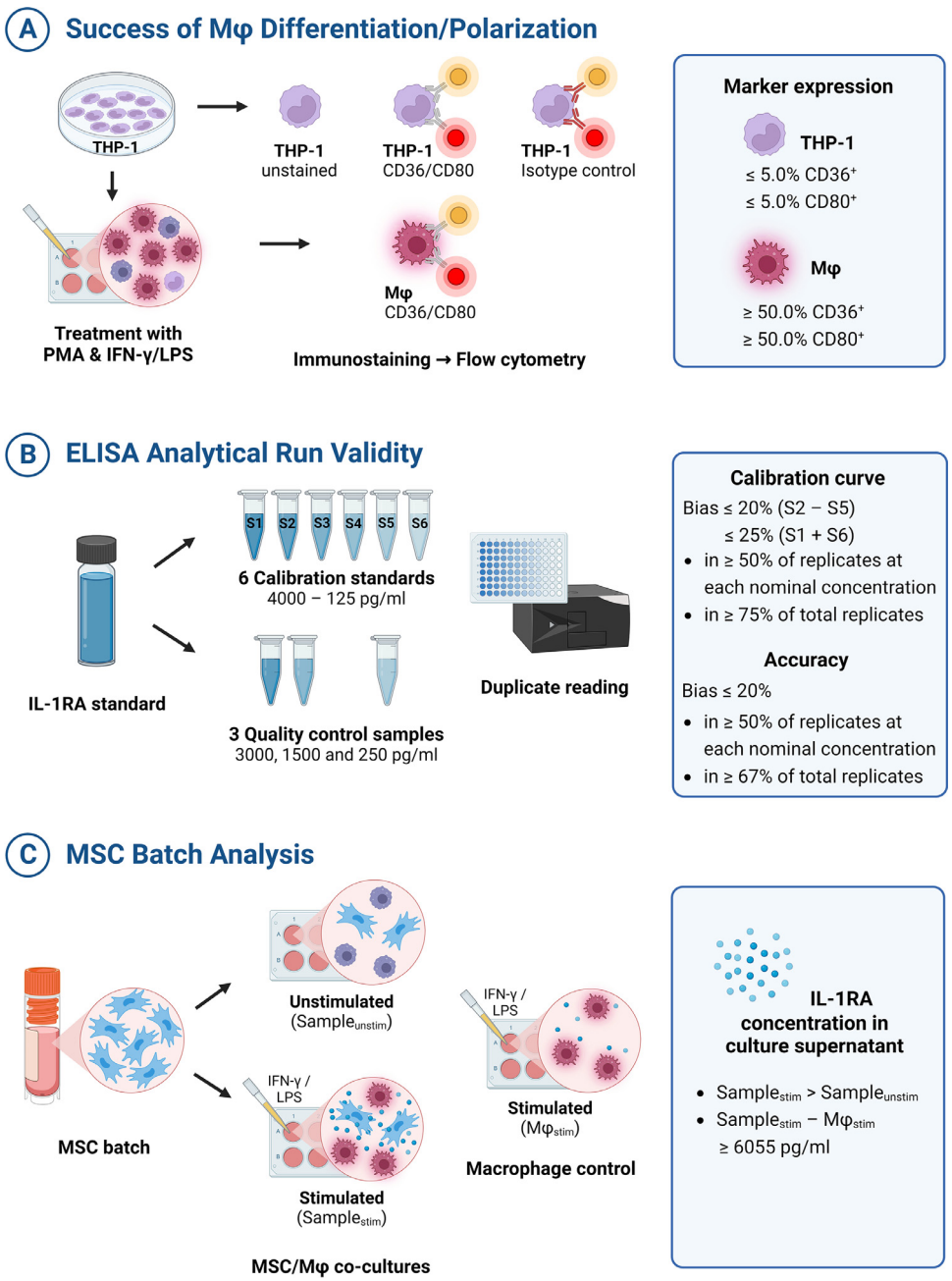

Fig. 4. Procedures and acceptance criteria of the IL-1RA potency assay for routine batch release. (A) Confirmation of macrophage differentiation and M1 polarization of THP-1 monocyte-derived macrophages (Mφ) by flow cytometric determination of the macrophage differentiation marker CD36 and the M1 polarization marker CD80. Successful differentiation/polarization is assumed if at least 50% of treated cells express both markers. Untreated THP-1 cells are used as controls and must not contain more than 5% of cells expressing both markers. (B) Validation of analytical IL-1RA ELISA runs according to the EMA's and FDA's guidelines on bioanalytical method validation [51–54]. (C) Assessment of the potency of ABCB5$^+$ MSCs to secrete IL-1RA in response to interferon IFN-γ/LPS-stimulated macrophages by ELISA determination of the IL-1RA concentration in the culture supernatant. An ABCB5$^+$ MSC batch is released only if the IL-1RA concentration exceeds that of unstimulated MSC/macrophage cocultures and if the total IL-1RA concentration minus the IL-1RA concentration measured in a parallel culture of stimulated macrophages without ABCB5$^+$ MSCs is at least 6055 pg/mL. Created with BioRender.com. (Color version of figure is available online.)

MSC product [9]. However, macrophage numbers observed *in vivo* can be highly variable depending on the target tissue and the type, stage and severity of the underlying disease [62], making it difficult to define expected therapeutic ratios. On the other hand, to meet the requirements for a potency assay as summarized above, it is not required to demonstrate that the strength of effect of a cell therapy product in the assay is identical to the strength of a clinically effective response seen with the product in vivo under therapeutic conditions. Rather, a potency assay is required to ensure that, under reproducible conditions, each released batch exerts, at a reasonably predefined level, a specific property or capability relevant to the product's mode of action. For these reasons, we sought to determine an MSC/macrophage ratio at which the IL-1RA secretion by the MSCs is maximally stimulated. By extensively testing the influence of a wide range of different MSC/macrophage ratios on IL-1RA secretion by the MSCs, we observed a linear relationship between MSC/macrophage ratio and IL-1RA secretion per MSC at MSC/macrophage ratios up to 1:50. Above this ratio, a flattening of the ratio-response curve indicated that the secretion output of the MSCs was approaching its maximum (Figure 3E, F). This suggested that saturation of the MSCs with their stimulators had been reached. Therefore, by selecting an MSC/macrophage ratio of 1:50 for batch release testing, the IL-1RA secretion

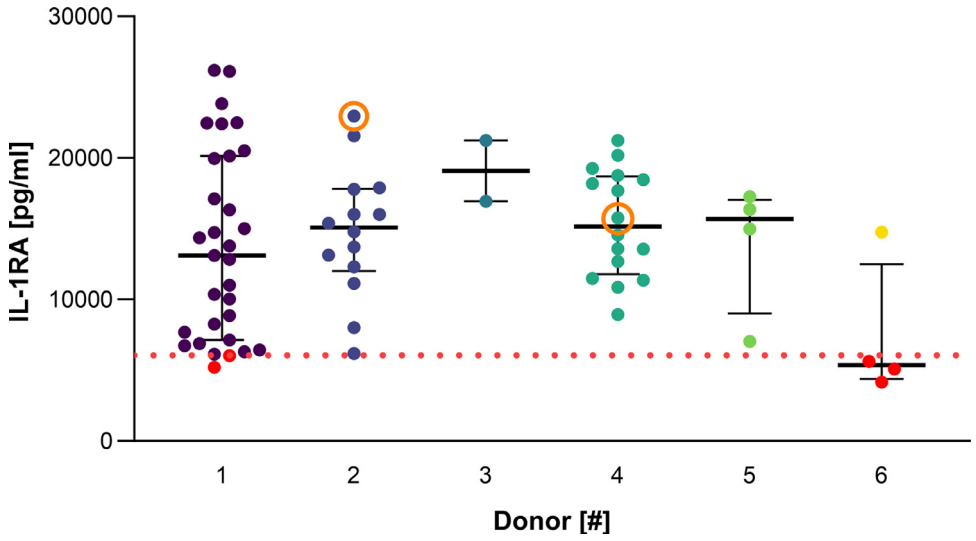

Fig. 5. Results from routine batch release testing showing IL-1RA secretion by ABCB5$^+$ MSCs in cocultures with THP-1-derived macrophages stimulated with IFN γ and LPS at an MSC/macrophage ratio of 1:50. Shown is the IL-1RA concentration measured in the coculture supernatant after subtracting the IL-1RA concentration measured in the culture supernatant of control cultures of stimulated macrophages cultured without ABCB5$^+$ MSCs. Data are from 71 MSC batches manufactured from skin tissues from six donors. Error bars show donor medians and interquartile ranges. The dotted line marks the acceptance level (6055 pg/mL) for batch release; batches that failed the acceptance criterion are colored in red. Kruskal-Wallis test followed by Dunn's multiple comparisons test revealed no statistically significant differences between donors. In addition to the IL-1RA secretion assay, all batches underwent a VEGF secretion assay under hypoxic culture conditions and an *in vitro* tube formation assay. All batches passed the tube formation assay, and all but two batches (failed batches are circled in orange) passed the VEGF secretion assay. (Color version of figure is available online.)

capacity of (near) maximally stimulated MSCs can be measured. In this way, the absolute maximum amount of secreted IL-1RA per individual MSC, and thus the maximum potency of the corresponding cell batch, can be quantified, allowing comparisons between cell batches and correlations between cell batches and the clinical results obtained with them.

One of the most challenging tasks in establishing a potency assay is setting the acceptance level for product batch release. In principle, regulators are proposing a stepwise approach depending on the stage of development of the cell therapy product [14]. This means that during earlier phases of clinical development, it is accepted to set acceptance criteria based on actual measured values of a suitable number of consecutive final batches. At this stage, the main focus is on ensuring batch-to-batch consistency and rejecting batches that are not behaving normally. With progress in clinical trials and increasing availability of clinical efficacy data, the acceptance criteria are to be adjusted to provide reasonable confidence that each product batch released will perform as expected. The herein applied acceptance level was set up based on earlier data from 25 batches of ABCB5$^+$ MSCs (supplemental Figure 1). To limit potential batch-to-batch variability, an acceptance threshold of 6055 pg/mL for IL-1RA secretion was defined as $\geq$ 70% of the median of 8650 pg/mL observed across these batches. Applying this threshold, 9 out of the 36 batches (28%) had to be rejected. In the course of GMP-compliant continuous refinement of the cell manufacturing process, only 7% (5 of 71, Figure 5) batches are currently rejected for failure to meet the release criterion for IL-1RA secretion. In line with the stepwise approach proposed by the regulatory authorities, which requires continuous adaptation and clinical justification of the acceptance criteria as product development progresses, we will adjust the acceptance level based on retrospective comparisons of the IL-1RA secretion data with the corresponding efficacy data that are generated in ongoing and future phase 2b and phase 3 clinical trials.

The general robustness and reproducibility of the potency assay was confirmed by batch release testing of 71 consecutively manufactured MSC batches (Figure 5), which showed a low overall failure rate (7%) and a high comparability between 5 out of 6 donors, confirming previous observations made with a preliminary qualitative IL-1RA secretion assay [39]. In contrast to these 5 donors, donor 6 had a high failure rate (75%), reflected by a median IL-1RA concentration below the acceptance level for batch release. As this was already evident after testing only four batches, the potency assay described here may not only be a suitable quality control measure, but also a useful tool for the early identification of potentially ineligible donors.

It is clear that a single potency assay that reflects a single mechanism of action cannot adequately predict the therapeutic functionality of an MSC-based medicinal product. This is because the regenerative potential of MSCs is based on multiple different properties including several immunomodulatory and trophic pathways that act together to restore homeostasis and facilitate regenerative responses in inflamed, injured or diseased tissues [16,63,64]. To obtain a more comprehensive picture under routine manufacturing conditions, the drug release potency assessment of ABCB5$^+$ MSCs includes, in addition to the IL-1RA secretion assay described here, a vascular endothelial growth factor (VEGF) secretion assay under hypoxic culture conditions to display the proangiogenic bioactivity in ischemic tissues and an *in vitro* tube formation assay to estimate the blood vessel-forming capacity of each cell batch produced [29,35,39]. Of the 71 consecutively manufactured batches, all met the criteria for successful tube formation, and all but two batches passed the VEGF secretion assay (Figure 5). No batch failed both the IL-1RA and VEGF assays, which was not expected since these assays represent two different modes of action. Importantly, only ABCB5$^+$ MSC batches that meet the specifications for all three potency assays are released for clinical use.

Conclusions

The present report describes the development and validation of a therapeutically relevant, straightforward, robust and reproducible *in vitro* potency assay to measure the anti-inflammatory capacity of culture-expanded MSCs in an M1 macrophage-dominated inflammatory environment by quantifying the amount of IL-1RA released by the MSCs in coculture with THP-1 monocyte-derived M1-polarized macrophages. Meeting the criteria required by drug-regulatory authorities, including: indicating product-specific biological activity,

providing quantitative data, meeting predefined acceptance/rejection criteria, and establishing and documenting the accuracy, sensitivity, specificity and reproducibility of the assay methods employed, the IL-1RA secretion assay has been implemented as an integral part of the quality control and release testing matrix of GMP-compliantly manufactured medicinal products based on skin-derived ABCB5$^+$ MSCs. The insights into the hurdles encountered and how they were overcome may be helpful to other cell therapy developers facing the challenge of selecting and establishing product-specific potency assays.

Declaration of Competing of interest

MHF is inventor or coinventor of U.S. and international patents assigned to Brigham and Women's Hospital and/or Boston Children's Hospital, licensed to RHEACELL GmbH & Co. KG. MHF and KS-K serve as scientific advisors to RHEACELL. MHF holds stock in RHEACELL. SS, LN, EN-R, AN, SH, LV and JE are employees of RHEACELL. CG is CEO, and MAK is COO of RHEACELL.

Funding

Contributions by MHF to this work were supported by the NIH/National Eye Institute (NEI) grants RO1EY025794 and R24EY028767, NIH National Heart, Lung, and Blood Institute (NHLBI) grant R01HL161087, and NIH National Institute on Aging P01AG071463. The funding sources had no involvement in study design; in the collection, analysis and interpretation of data; in the writing of the report; and in the decision to submit the article for publication.

Author Contributions

Conception and design of the study: SS, LN, AN, SH, JE, MHF, CG, KS-K, MAK, Acquisition of data: LN, AN, SH, LV, Analysis and interpretation of data: SS, LN, EN-R, AN, SH, LV, JE , Drafting the manuscript: EN-R, Revising the manuscript: SS, LN, EN-R, AN, SH, LV, JE, MHF, CG, KS-K, MAK, All authors have approved the final article.

Ethics Statement

This article does not contain any studies involving animal or human subjects. ABCB5$^+$ MSCs were derived from human skin samples that were collected in accordance with the German Medicines Act ("Arzneimittelgesetz") and the German Act on Organ and Tissue Donation, Removal and Transplantation ("Transplantationsgesetz") as waste tissues from plastic surgery procedures from donors who had given written informed consent.

Supplementary materials

Supplementary material associated with this article can be found in the online version at doi:10.1016/j.jcyt.2024.02.004.

References

[1] Gómez-Cid L, Grigorian-Shamagian L, Sanz-Ruiz R, de la Nava AS, Fernández AI, Fernández-Santos ME, et al. The essential need for a validated potency assay for cell-based therapies in cardiac regenerative and reparative medicine. a practical approach to test development. Stem Cell Rev Rep 2021;17:2235–44.
[2] Hansen SB, Højgaard LD, Kastrup J, Ekblond A, Follin B, Juhl M. Optimizing an immunomodulatory potency assay for mesenchymal stromal cell. Front Immunol 2022;13:1085312.
[3] Wang T, Zhang J, Liao J, Zhang F, Zhou G. Donor genetic backgrounds contribute to the functional heterogeneity of stem cells and clinical outcomes. Stem Cells Transl Med 2020;9:1495–9.
[4] Wang YH, Tao YC, Wu DB, Wang ML, Tang H, Chen EQ. Cell heterogeneity, rather than the cell storage solution, affects the behavior of mesenchymal stem cells in vitro and in vivo. Stem Cell Res Ther 2021;12:391.
[5] Costa LA, Eiro N, Fraile M, Gonzalez LO, Saá J, Garcia-Portabella P, et al. Functional heterogeneity of mesenchymal stem cells from natural niches to culture conditions: implications for further clinical uses. Cell Mol Life Sci 2021;78:447–67.
[6] Dunn CM, Kameishi S, Grainger DW, Okano T. Strategies to address mesenchymal stem/stromal cell heterogeneity in immunomodulatory profiles to improve cell-based therapies. Acta Biomater 2021;133:114–25.
[7] Olmedo-Moreno L, Aguilera Y, Baliña-Sánchez C, Martín-Montalvo A, Capilla-González V. Heterogeneity of in vitro expanded mesenchymal stromal cells and strategies to improve their therapeutic actions. Pharmaceutics 2022;14:1112.
[8] Salmikangas P, Carlsson B, Klumb C, Reimer T, Thirstrup S. Potency testing of cell and gene therapy products. Front Med (Lausanne) 2023;10:1190016.
[9] de Wolf C, van de Bovenkamp M, Hoefnagel M. Regulatory perspective on in vitro potency assays for human mesenchymal stromal cells used in immunotherapy. Cytotherapy 2017;19:784–97.
[10] Lowdell MW, Weil B. Bringing function to the forefront of cell therapy: how do we demonstrate potency? Front Immunol 2023;14:1226841.
[11] Galipeau J, Krampera M, Barrett J, Dazzi F, Deans RJ, DeBruijn J, et al. International Society for Cellular Therapy perspective on immune functional assays for mesenchymal stromal cells as potency release criterion for advanced phase clinical trials. Cytotherapy 2016;18:151–9.
[12] European Medicines Agency, Guideline on human cell-based medicinal products (EMEA/CHMP/410869/2006), 2008. https://www.ema.europa.eu/en/documents/scientific-guideline/guideline-human-cell-based-medicinal-products_en.pdf. [accessed 14.11.23].
[13] European Medicines Agency, Guideline on potency testing of cell based immunotherapy medicinal products for the treatment of cancer (EMEA/CHMP/BWP/271475/2006 rev. 1), 2016. https://www.ema.europa.eu/en/documents/scientific-guideline/guideline-potency-testing-cell-based-immunotherapy-medicinal-products-treatment-cancer-revision-1_en.pdf. [accessed 14.11.23].
[14] U.S. Food and Drug Administration, Center for biologics evaluation and research, guidance for industry: potency tests for cellular and gene therapy products, 2011. https://www.fda.gov/media/79856/download. [accessed 14.11.23].
[15] Müller L, Tunger A, Wobus M, von Bonin M, Towers R, Bornhäuser M, et al. Immunomodulatory properties of mesenchymal stromal cells: an update. Front Cell Dev Biol 2021;9:637725.
[16] Alvites R, Branquinho M, Sousa AC, Lopes B, Sousa P, Maurício AC. Mesenchymal stem/stromal cells and their paracrine activity-immunomodulation mechanisms and how to influence the therapeutic potential. Pharmaceutics 2022;14:381.
[17] Huang Y, Wu Q, Tam PKH. Immunomodulatory mechanisms of mesenchymal stem cells and their potential clinical applications. Int J Mol Sci 2022;23:10023.
[18] Li P, Ou Q, Shi S, Shao C. Immunomodulatory properties of mesenchymal stem cells/dental stem cells and their therapeutic applications. Cell Mol Immunol 2023;20:558–69.
[19] Krampera M, Galipeau J, Shi Y, Tarte K, Sensebe L. Immunological characterization of multipotent mesenchymal stromal cells: the International Society for Cellular Therapy (ISCT) working proposal. Cytotherapy 2013;15:1054–61.
[20] Capelli C, Cuofano C, Pavoni C, Frigerio S, Lisini D, Nava S, et al. Potency assays and biomarkers for cell-based advanced therapy medicinal products. Front Immunol 2023;14:1186224.
[21] Oliver-Vila I, Ramírez-Moncayo C, Grau-Vorster M, Marín-Gallén S, Caminal M, Vives J. Optimisation of a potency assay for the assessment of immunomodulative potential of clinical grade multipotent mesenchymal stromal cells. Cytotechnology 2018;70:31–44.
[22] Robb KP, Fitzgerald JC, Barry F, Viswanathan S. Mesenchymal stromal cell therapy: progress in manufacturing and assessments of potency. Cytotherapy 2019;21:289–306.
[23] Kebriaei P, Isola L, Bahceci E, Holland K, Rowley S, McGuirk J, et al. Adult human mesenchymal stem cells added to corticosteroid therapy for the treatment of acute graft-versus-host disease. Biol Blood Marrow Transplant 2009;15:804–11.
[24] Kurtzberg J, See F, Burke E, Hayes J. The immunomodulatory activity of remestemcel-L on T cell activation in vitro is a direct measure of product potency and correlates with clinical outcomes in pediatric patients with steroid-refractory acute Gvhd. In: Presented at the Transplantation & Cellular Therapy Meetings of ASTCT and CIBMTR, February 15-19, 2023, Orlando, Florida, USA; 2023. https://tandem.confex.com/tandem/2023/meetingapp.cgi/Paper/22428 [accessed 14.11.23].
[25] Kuçi Z, Bönig H, Kreyenberg H, Bunos M, Jauch A, Janssen JW, et al. Mesenchymal stromal cells from pooled mononuclear cells of multiple bone marrow donors as rescue therapy in pediatric severe steroid-refractory graft-versus-host disease: a multicenter survey. Haematologica 2016;101:985–94.
[26] Piede N, Bremm M, Farken A, Pfeffermann LM, Cappel C, Bonig H, et al. Validation of an ICH Q2 compliant flow cytometry-based assay for the assessment of the inhibitory potential of mesenchymal stromal cells on T cell proliferation. Cells 2023;12:850.
[27] Ren G, Peng Q, Fink T, Zachar V, Porsborg SR. Potency assays for human adipose-derived stem cells as a medicinal product toward wound healing. Stem Cell Res Ther 2022;13:249.
[28] Krampera M, Le Blanc K. Mesenchymal stromal cells: putative microenvironmental modulators become cell therapy. Cell Stem Cell 2021;28:1708–25.
[29] Niebergall-Roth E, Frank NY, Ganss C, Frank MH, Kluth MA. Skin-derived ABCB5 (+) mesenchymal stem cells for high-medical-need inflammatory diseases: from discovery to entering clinical routine. Int J Mol Sci 2022;24:66.
[30] Vander Beken S, de Vries JC, Meier-Schiesser B, Meyer P, Jiang D, Sindrilaru A, et al. Newly defined ATP-binding cassette subfamily B member 5 positive dermal mesenchymal stem cells promote healing of chronic iron-overload wounds via secretion of interleukin-1 receptor antagonist. Stem Cells 2019;37:1057–74.

[31] Webber BR, O'Connor KT, McElmurry RT, Durgin EN, Eide CR, Lees CJ, et al. Rapid generation of Col7a1(-/-) mouse model of recessive dystrophic epidermolysis bullosa and partial rescue via immunosuppressive dermal mesenchymal stem cells. Lab Invest 2017;97:1218–24.
[32] Singh K, Maity P, Koroma AK, Basu A, Pandey RK, Vander Beken S, et al. Angiogenin released from ABCB5(+) stromal precursors improves healing of diabetic wounds by promoting angiogenesis. J Invest Dermatol 2022;142: 1725–36.
[33] Kerstan A, Niebergall-Roth E, Esterlechner J, Schröder HM, Gasser M, Waaga-Gasser AM, et al. Ex vivo-expanded highly pure ABCB5(+) mesenchymal stromal cells as good manufacturing practice-compliant autologous advanced therapy medicinal product for clinical use: process validation and first in-human data. Cytotherapy 2021;23:165–75.
[34] Kerstan A, Dieter K, Niebergall-Roth E, Dachtler A-K, Kraft K, Stücker M, et al. Allogeneic ABCB5(+) mesenchymal stem cells for treatment-refractory chronic venous ulcers: a phase I/IIa clinical trial. JID Innovations 2022;2:100067.
[35] Kerstan A, Dieter K, Niebergall-Roth E, Klingele S, Jünger M, Hasslacher C, et al. Translational development of ABCB5+ dermal mesenchymal stem cells for therapeutic induction of angiogenesis in non-healing diabetic foot ulcers. Stem Cell Res Ther 2022;13:455.
[36] Kiritsi D, Dieter K, Niebergall-Roth E, Fluhr S, Daniele C, Esterlechner J, et al. Clinical trial of ABCB5+ mesenchymal stem cells for recessive dystrophic epidermolysis bullosa. JCI Insight 2021;6:e151922.
[37] Dieter K, Niebergall-Roth E, Daniele C, Fluhr S, Frank NY, Ganss C, et al. ABCB5(+) mesenchymal stromal cells facilitate complete and durable wound closure in recessive dystrophic epidermolysis bullosa. Cytotherapy 2023;25:782–8.
[38] Niebergall-Roth E, Dieter K, Daniele C, Fluhr S, Khokhrina M, Silva I, et al. Kinetics of wound development and healing suggests a skin-stabilizing effect of allogeneic ABCB5(+) mesenchymal stromal cell treatment in recessive dystrophic epidermolysis bullosa. Cells 2023;12:1468.
[39] Ballikaya S, Sadeghi S, Niebergall-Roth E, Nimtz L, Frindert J, Norrick A, et al. Process data of allogeneic ex vivo-expanded ABCB5+ mesenchymal stromal cells for human use: off-the-shelf GMP-manufactured donor-independent ATMP. Stem Cell Res Ther 2020;11:482.
[40] Alessio M, De Monte L, Scirea A, Gruarin P, Tandon NN, Sitia R. Synthesis, processing, and intracellular transport of CD36 during monocytic differentiation. J Biol Chem 1996;271:1770–5.
[41] Hayden JM, Brachova L, Higgins K, Obermiller L, Sevanian A, Khandrika S, et al. Induction of monocyte differentiation and foam cell formation in vitro by 7-ketocholesterol. J Lipid Res 2002;43:26–35.
[42] Al-Rasheed NM, Chana RS, Baines RJ, Willars GB, Brunskill NJ. Ligand-independent activation of peroxisome proliferator-activated receptor-gamma by insulin and C-peptide in kidney proximal tubular cells: dependent on phosphatidylinositol 3-kinase activity. J Biol Chem 2004;279:49747–54.
[43] Viñals M, Bermúdez I, Llaverias G, Alegret M, Sanchez RM, Vázquez-Carrera M, et al. Aspirin increases CD36, SR-BI, and ABCA1 expression in human THP-1 macrophages. Cardiovasc Res 2005;66:141–9.
[44] Phillips RJ, Lutz M, Premack B. Differential signaling mechanisms regulate expression of CC chemokine receptor-2 during monocyte maturation. J Inflamm (Lond) 2005;2:14.
[45] Rios FJ, Jancar S, Melo IB, Ketelhuth DF, Gidlund M. Role of PPAR-gamma in the modulation of CD36 and FcgammaRII induced by LDL with low and high degrees of oxidation during the differentiation of the monocytic THP-1 cell line. Cell Physiol Biochem 2008;22:549–56.
[46] Maess MB, Sendelbach S, Lorkowski S. Selection of reliable reference genes during THP-1 monocyte differentiation into macrophages. BMC Mol Biol 2010;11:90.
[47] Zhou L, Shen LH, Hu LH, Ge H, Pu J, Chai DJ, et al. Retinoid X receptor agonists inhibit phorbol-12-myristate-13-acetate (PMA)-induced differentiation of monocytic THP-1 cells into macrophages. Mol Cell Biochem 2010;335:283–9.
[48] Chanput W, Mes JJ, Wichers HJ. THP-1 cell line: an in vitro cell model for immune modulation approach. Int Immunopharmacol 2014;23:37–45.
[49] Genin M, Clement F, Fattaccioli A, Raes M, Michiels C. M1 and M2 macrophages derived from THP-1 cells differentially modulate the response of cancer cells to etoposide. BMC Cancer 2015;15:577.
[50] Forrester MA, Wassall HJ, Hall LS, Cao H, Wilson HM, Barker RN, et al. Similarities and differences in surface receptor expression by THP-1 monocytes and differentiated macrophages polarized using seven different conditioning regimens. Cell Immunol 2018;332:58–76.
[51] European Medicines Agency, Guideline on bioanalytical method validation (EMEA/CHMP/EWP/192217/2009 Rev. 1 Corr. 2), 2011. https://www.ema.europa.eu/en/documents/scientific-guideline/guideline-bioanalytical-method-validation_en.pdf. [accessed 14.11.23].
[52] U.S. Food and Drug Administration, Center for drug evaluation and research & center for veterinary medicine, bioanalytical method validation: guidance for industry, 2018. https://www.fda.gov/files/drugs/published/Bioanalytical-Method-Validation-Guidance-for-Industry.pdf. [accessed 14.11.23].
[53] European Medicines Agency, ICH guideline M10 on bioanalytical method validation and study sample analysis (EMEA/CHMP/ICH/172948/2019), 2022. https://www.ema.europa.eu/en/documents/scientific-guideline/ich-guideline-m10-bioanalytical-method-validation-step-5_en.pdf. [accessed 14.11.23].
[54] U.S. Food and Drug Administration, Center for drug evaluation and research & center for biologics evaluation and research, M10 bioanalytical method validation and study sample analysis: guidance for industry, 2022. https://www.fda.gov/media/162903/download. [accessed 14.11.23].
[55] Pimpaneau V, Gianelli F, Trouvin J-H, Poiseau AD. The challenges of potency assay development for cell-based medicinal products in Europe. Regul Rapporteur 2015;12:5–10.
[56] Sindrilaru A, Scharffetter-Kochanek K. Disclosure of the culprits: macrophages-versatile regulators of wound healing. Adv Wound Care (New Rochelle) 2013; 2:357–68.
[57] Tedesco S, De Majo F, Kim J, Trenti A, Trevisi L, Fadini GP, et al. Convenience versus biological significance: are PMA-differentiated THP-1 cells a reliable substitute for blood-derived macrophages when studying in vitro polarization? Front Pharmacol 2018;9:71.
[58] Hoppenbrouwers T, Bastiaan-Net S, Garssen J, Pellegrini N, Willemsen LEM, Wichers HJ. Functional differences between primary monocyte-derived and THP-1 macrophages and their response to LCPUFAs. PharmaNutrition 2022;22:100322.
[59] Dhakal B, Li CMY, Ramezanpour M, Houtak G, Li R, Bouras G, et al. Proteomic characterisation of perhexiline treatment on THP-1 M1 macrophage differentiation. Front Immunol 2023;14:1054588.
[60] He F, Umrath F, Reinert S, Alexander D. Jaw periosteum-derived mesenchymal stem cells regulate THP-1-derived macrophage polarization. Int J Mol Sci 2021;22:4310.
[61] Liu L, Shi W, Xiao X, Wu X, Hu H, Yuan S, et al. BCG immunotherapy inhibits cancer progression by promoting the M1 macrophage differentiation of THP-1 cells via the Rb/E2F1 pathway in cervical carcinoma. Oncol Rep 2021;46:245.
[62] Ross EA, Devitt A, Johnson JR. Macrophages: the good, the bad, and the gluttony. Front Immunol 2021;12:708186.
[63] Jimenez-Puerta GJ, Marchal JA, López-Ruiz E, Gálvez-Martín P. Role of mesenchymal stromal cells as therapeutic agents: potential mechanisms of action and implications in their clinical use. J Clin Med 2020;9:445.
[64] Fu Y, Karbaat L, Wu L, Leijten J, Both SK, Karperien M. Trophic effects of mesenchymal stem cells in tissue regeneration. Tissue Eng Part B Rev 2017;23:515–28.